Correlated Noise Estimation with Quantum Sensor Networks

Anthony J. Brady,[1,2,*] Yu-Xin Wang (王语馨),[1] Victor V. Albert,[1] Alexey V. Gorshkov,[1,2] and Quntao Zhuang[3,4]

[1] *Joint Center for Quantum Information and Computer Science, NIST/University of Maryland, College Park, MD, 20742, USA*

[2] *Joint Quantum Institute, NIST/University of Maryland, College Park, MD, 20742, USA*

[3] *Ming Hsieh Department of Electrical and Computer Engineering, University of Southern California, Los Angeles, CA 90089, USA*

[4] *Department of Physics and Astronomy, University of Southern California, Los Angeles, CA 90089, USA*

(Dated: December 27, 2024)

In this article, we address the metrological problem of estimating collective stochastic properties of a many-body quantum system. Canonical examples include center-of-mass quadrature fluctuations in a system of bosonic modes and correlated dephasing in an ensemble of qubits (e.g., spins) or fermions. We develop a theoretical framework to determine the limits of correlated (weak) noise estimation with quantum sensor networks and unveil the requirements for entanglement advantage. Notably, an advantage emerges from the synergistic interplay between *quantum* correlations of the sensors and *classical* (spatial) correlations of the noises. We determine optimal entangled probe states and identify a sensing protocol—reminiscent of a many-body echo sequence—that achieves the fundamental limits of measurement sensitivity for a broad class of problems.

Introduction.—Quantum metrology is one of the most promising areas of quantum information science [1, 2], dedicated to estimating parameters encoded in the quantum state of a physical system, such as a spin (qubit), photonic mode, or mechanical oscillator. Employing quantum systems as sensors [3] and engineering special probe states—such as Greenberger–Horne–Zeilinger (GHZ) states, spin-squeezed states, and squeezed vacuum states—enables estimation with precision surpassing that of classical methods.

For instance, when estimating the parameter ϑ encoded in a quantum system through a unitary process, $\hat{U}_\vartheta = e^{-i\vartheta\hat{h}}$, the Heisenberg limit, $\mathrm{Var}(\vartheta) \propto 1/\nu^2$, establishes the ultimate precision bound, attainable via entangled quantum probes given ν copies of the unitary, $\hat{U}_\vartheta^{\otimes\nu}$ [2]. Here $\mathrm{Var}(\vartheta)$ denotes the mean squared error. This contrasts with typical shot-noise scaling, $\mathrm{Var}(\vartheta) \propto 1/\nu$, attainable via independent experiments and separable (non-entangled) quantum probes [1, 2]. Prominent examples of unitary parameter estimation include: estimating the phase of a two-level system (e.g., a spin or qubit) for precision timing [4–7]; estimating the phase of a bosonic mode for interferometry [8–11]; estimating the displacement of an oscillator [12, 13] for gravitational wave astronomy [14–16]; and many-body Hamiltonian learning [17–20].

Quantum sensor networks (QSNs) represent a distinct paradigm of quantum metrology in which we aim to estimate, e.g., a collective property of the QSN, such as a linear combination of local parameters. Entanglement between K quantum sensors facilitates an enhancement, i.e., Heisenberg scaling with K, for such aggregate queries [21–28]. Examples include distributed versions of the standard estimation problems, featuring a network of quantum clocks [29–32], networked optical interferometry [25, 33, 34], and collective displacement sensing [24, 35–37].

Apart from unitary parameter estimation, estimating stochastic (or noise) properties is equally important. Canonical examples include stochastic versions of classic unitary problems: spin dephasing [38, 39], bosonic dephasing [40], and random displacement sensing [41–45] to name a few [46]; see also the related topic of multi-qubit noise characterization [47, 48]. Noise estimation fundamentally differs from unitary parameter estimation, presenting its own distinct challenges and techniques [39] (see also Refs. [38, 49–55]). For instance, given ν identical and independent copies of a noise channel, $\Phi_\vartheta^{\otimes\nu}$, the estimation precision of ϑ is typically constrained to shot-noise scaling with ν [49, 51]. However, insights about independent noise channels do not always translate to scenarios involving correlated noise (even in the context of unitary estimation under noisy dynamics [56]).

A key open question arises: Under what circumstances can we expect an entanglement advantage when estimating (spatially) correlated stochastic properties with QSNs, and how might we achieve this? Positive answers in this direction have implications for various fields—such as searching for new physics with quantum sensors [57–61], collective force [36, 62] or electric field sensing [37, 63], physical-layer supervised learning with QSNs [64, 65], and more broadly, metrological aspects of many-body quantum systems [66, 67].

In this work, we develop a theoretical framework for estimating correlated stochastic processes with QSNs. Our analysis reveals that, given a single copy of a K-sensor noise channel, classical spatial correlations between the noise processes at different sensor sites prove crucial for an entanglement advantage in estimation. Physically, the QSN may consist of qubits, fermions, or bosons. Nonetheless, our major findings are agnostic to the composition of the systems and, thus, apply broadly. To

* ajbrad4123@gmail.com

illustrate this versatility, we present concrete examples where an entanglement advantage in correlated noise estimation emerges: including correlated spin, bosonic, and fermionic dephasing and random bosonic displacements.

Problems in estimating correlated spin dephasing [68–71] and random displacements [59, 62] (cf. Supplementary Note 6 of Ref. [43]) have been partially explored. However, the problem of estimating collective bosonic dephasing, to the best of our knowledge, has not been addressed, particularly in the energy-constrained setting. Recently, Huang et al [40] studied estimation of single-mode bosonic dephasing at infinite energy. Our results on weak dephasing at finite energy, together with Ref. [40], sketch a more complete picture of the problem.

Theoretical framework.—Consider K quantum sensors comprising a QSN, and associate to each sensor a local (Hermitian) generator $\hat{h}_j$ $(j = 1, \ldots, K)$. For concreteness, we assume only one generator per sensor, so that all generators commute. Suppose the local generator $\hat{h}_j$ induces the translation, $\lambda_j \in \mathbb{R}$, on the jth sensor, and let the set of translations $\{\lambda_j\}_{j=1}^K$ be multivariate (e.g., Gaussian) random variables. We prioritize noise estimation and henceforth take $\mathbb{E}[\lambda_j] = 0, \forall j$. The translations thus correspond to (weak) fluctuations, which we package into the $K \times K$ covariance matrix, $\boldsymbol{V} > 0$, with elements $\boldsymbol{V}_{ij} = \mathbb{E}[\lambda_i \lambda_j]$. [We disregard higher-order moments, presuming they are parametrically weaker.] Generally, there exist correlations between the translations at different sensors due to classically shared randomness.

Let $\rho \in \mathscr{H}^{\otimes K}$ denote the QSN probe state, where $\mathscr{H}$ symbolizes the Hilbert space of a single sensor. The quantum channel $\Phi_{\boldsymbol{V}}$ encodes the fluctuations $\boldsymbol{V}$ onto the probe via $\Phi_{\boldsymbol{V}}(\rho)$. A crucial assumption we use in this work is that the encoded state admits the approximate form

$$\Phi_{\boldsymbol{V}}(\rho) \approx \rho + \sum_{i,j=1}^{K} \boldsymbol{V}_{ij} \left(\hat{h}_i \rho \hat{h}_j - \frac{1}{2} \left\{ \hat{h}_i \hat{h}_j, \rho \right\} \right). \tag{1}$$

Intuitively, this can be understood as representing many-body open-system dynamics within the Markov regime, where $\hat{h}_j$ are local jump operators and $\boldsymbol{V}_{ij} = \boldsymbol{\gamma}_{ij} \Delta t$, with $\boldsymbol{\gamma}_{ij}$ denoting many-body decoherence rates and Δt an infinitesimal time interval. This yields $\rho = \rho(t)$ and $\Phi_{\boldsymbol{V}}(\rho) = \rho(t + \Delta t)$. Alternatively, the expansion may describe weak, random unitary evolution where the unitary $\bigotimes_{j=1}^{K} e^{-i\lambda_j \hat{h}_j}$ acts according to probability $p(\lambda_1, \ldots, \lambda_K)$, with zero mean and covariance $\boldsymbol{V}$. In this interpretation, the expansion is with respect to a small parameter $\varepsilon \ll 1$ such that $\mathbb{E}[\vec{\lambda}_{i_1} \ldots \vec{\lambda}_{i_n} \hat{h}_{i_1} \ldots \hat{h}_{i_n}] \sim \varepsilon^n$ $(n \geq 2)$. See Appendix A for further discussion.

We aim to estimate a collection of n aggregate (or non-local) parameters, $\Theta \coloneqq \{\vartheta_J\}_{J=1}^n$. For concreteness, we concentrate on two settings where these parameters may arise: (i) The parameters are directly embedded into the covariance matrix, $\boldsymbol{V}(\Theta)$, thereby controlling the elements of $\boldsymbol{V}$ (cf. [21, 27]). (ii) The parameters are constructed from non-trivial combinations of the $\boldsymbol{V}_{ij}$'s [e.g., $\vartheta_I^2(\boldsymbol{V}) = \sum_{i,j} (\vec{w}_I)_i (\vec{w}_I)_j \boldsymbol{V}_{ij}$ for some vector $\vec{w}_I$], without assuming explicit knowledge of $\boldsymbol{V}$ (cf. [22, 26, 72]). For clarity, we refer to these settings as case (i) and case (ii) throughout.

To address these estimation problems, we utilize the quantum theory of multi-parameter estimation [73–75]. Given the encoded quantum data, $\Phi_{\boldsymbol{V}}(\rho)$, we perform measurements and construct estimates, $\{\check{\vartheta}_J\}_{J=1}^n$, from the measurement statistics. We quantify the performance of the estimation procedure by the mean-squared error, $\mathrm{Var}(\vartheta_J) \coloneqq \mathbb{E}[(\check{\vartheta}_J - \vartheta_J)^2]$. Assuming an unbiased estimator, such that $\mathbb{E}[\check{\vartheta}_J] = \vartheta_J$, the quantum Fisher information (QFI) ultimately bounds the mean-squared error from below [73–75],

$$\mathrm{Var}(\vartheta_I) \geq \nu^{-1} (\boldsymbol{\mathcal{F}}_{\mathcal{Q}}^{-1}(\Theta))_{II} \geq \nu^{-1} (\boldsymbol{\mathcal{F}}_{\mathcal{Q}}(\Theta))_{II}^{-1}, \tag{2}$$

where $\boldsymbol{\mathcal{F}}_{\mathcal{Q}}(\Theta)$ is the QFI matrix for the parameter set Θ and ν denotes the number of independent repetitions. This bound does not necessarily guarantee achievability nor provide optimal measurement strategies, subjects that we examine in more detail later.

To compute the QFI matrix, we employ the geometric relation between $\boldsymbol{\mathcal{F}}_{\mathcal{Q}}$ and the fidelity of quantum states through the Bures distance [76]. Assuming Θ parametrize small perturbations to the identity channel, the Bures distance reads

$$\sum_{I,J=1}^{n} (\boldsymbol{\mathcal{F}}_{\mathcal{Q}}(\Theta))_{IJ} \, \vartheta_I \vartheta_J = 8 \left(1 - \sqrt{F(\rho, \rho_\vartheta)} \right), \tag{3}$$

where $\rho_\vartheta = \Phi_{\boldsymbol{V}}(\rho)$. Here, $F(\tau, \rho) = \mathrm{Tr}[\sqrt{\sqrt{\tau} \rho \sqrt{\tau}}]^2$ is the fidelity. We then employ the channel approximation (1) to expand the fidelity to leading order as $F(\rho, \rho_\vartheta) \approx 1 - \mathrm{Tr}\{\boldsymbol{V} \boldsymbol{\mathcal{H}}\}$, assuming $\mathrm{Tr}\{\boldsymbol{V} \boldsymbol{\mathcal{H}}\} \ll 1$ and a pure probe state (which maximizes the QFI through a convexity argument). This yields our main general result, which applies to cases (i) and (ii) mentioned previously and whose proof we relegate to Appendix B.

Result. *Consider the pure QSN probe $\rho = |\psi\rangle\langle\psi|$, and let $\boldsymbol{\mathcal{H}}$ denote the "Hamiltonian" generator matrix of ρ, with elements $\boldsymbol{\mathcal{H}}_{ij} = \langle \hat{h}_i \hat{h}_j \rangle - \langle \hat{h}_i \rangle \langle \hat{h}_j \rangle$. We deduce a direct relation between the QFI matrix $\boldsymbol{\mathcal{F}}_{\mathcal{Q}}(\Theta)$, the covariance matrix of the channel $\boldsymbol{V}$, and the generator matrix $\boldsymbol{\mathcal{H}}$,*

$$\sum_{I,J=1}^{n} (\boldsymbol{\mathcal{F}}_{\mathcal{Q}}(\Theta))_{IJ} \, \vartheta_I \vartheta_J \stackrel{!}{=} 4 \, \mathrm{Tr}\{\boldsymbol{V} \boldsymbol{\mathcal{H}}\}. \tag{4}$$

In words, the degree of classical, spatial correlations between the noise sources dictates whether an entanglement advantage manifests. On the one hand, when the noises share no spatial correlations, such that $\boldsymbol{V}_{ij} = V_i \delta_{ij}$, the QFI matrix depends solely on the local generator variances, $\boldsymbol{\mathcal{H}}_{ii} = \mathrm{Var}(\hat{h}_i)$, and entangled quantum probes bear no fruit. This aligns with established results in uncorrelated noise estimation [38, 77]. On the other hand, when significant spatial correlations between the noises exist, entanglement across the QSN affords enhanced precision for all types of random quantum processes.

Examples.— We first target a simple yet appealing class of problems that fall under case (i). Suppose $\boldsymbol{V}_{ij} = g^2\boldsymbol{v}_{ij}$, where $\boldsymbol{v}_{ij}$ are known. Physically, the numbers $\boldsymbol{v}_{ij}$ may be functions of device characteristics or geometrical functions that depend on the relative distances between the sensors, the distances from the sensors to the source of g etc. This is relevant in practical scenarios, where the sensor array has been characterized (masses, susceptibility functions etc. are known) and calibrated to, e.g., detect global random forces [36], electric fields [37, 63], or to search for new physics [57–62].

By consequence of Eq. (4), we obtain the following.

Corollary. *Suppose $\boldsymbol{V}_{ij} = g^2\boldsymbol{v}_{ij}$ with g an unknown parameter and $\boldsymbol{v}_{ij}$ known, the QFI for estimating g is*

$$\mathcal{F}_{\mathcal{Q}}(g) = 4\,\mathrm{Tr}\{\boldsymbol{v}\boldsymbol{\mathcal{H}}\}. \tag{5}$$

When $\boldsymbol{v}$ is rank 1 and permutation invariant (indicating maximally correlated noises), such that $\boldsymbol{v} = K\vec{u}\vec{u}^{\top}$ with $\vec{u} = (1, 1, \ldots, 1)^{\top}/\sqrt{K}$, we anticipate the largest possible entanglement advantage. To formalize this, define the network average generator, $\hat{H} \coloneqq \sum_{i=1}^{K} \hat{h}_i/K$. Then, per Eq. (5), we have

$$\mathcal{F}_{\mathcal{Q}}(g) = 4K^2\mathrm{Var}\big(\hat{H}\big). \tag{6}$$

For comparison, the QFI for separable probes reads $\mathcal{F}_{\mathcal{Q}}^{\mathrm{sep}}(g) = 4K(\sum_i \mathrm{Var}(\hat{h}_i)/K)$, which exhibits shot-noise scaling ($\propto K$). To achieve Heisenberg scaling ($\mathcal{F}_{\mathcal{Q}} \propto K^2$) with the QSN, we demand that $\mathrm{Var}(\hat{H}) \approx \mathrm{Var}(\hat{h})$, where $\mathrm{Var}(\hat{h})$ is a typical variance of the local generator. Since $\mathrm{Var}(\hat{H}) = (\sum_{i,j} \langle\hat{h}_i\hat{h}_j\rangle - \langle\hat{h}_i\rangle\langle\hat{h}_j\rangle)/K^2$, each term in the sum must be of order $\mathrm{Var}(\hat{h})$, which is possible via many-body quantum correlations of the probe. We illustrate this for prototypical noise processes.

Example 1. Consider qubit (or spin) dephasing with local generators $\hat{h}_i = \hat{Z}_i$, where $\hat{Z}_i$ is the Pauli-Z operator at the ith sensor. Define the average spin $\hat{Z}_{\mathrm{avg}} = \sum_{i=1}^{K} \hat{Z}_i/K$. For entangled and separable strategies, respectively, we find

$$\mathcal{F}_{\mathcal{Q}}^{\mathrm{ent}}(g) = 4K^2\mathrm{Var}\big(\hat{Z}_{\mathrm{avg}}\big) \leq 4K^2, \tag{7}$$

$$\mathcal{F}_{\mathcal{Q}}^{\mathrm{sep}}(g) = 4K\left(\sum_{i=1}^{K}\mathrm{Var}(\hat{Z}_i)/K\right) \leq 4K. \tag{8}$$

The optimal separable probe is the product state $((|{\downarrow}\rangle + |{\uparrow}\rangle)/\sqrt{2})^{\otimes K}$. The optimal entangled probe is the GHZ state, $(|{\downarrow\downarrow}\ldots\rangle + |{\uparrow\uparrow}\ldots\rangle)/\sqrt{2}$ (cf. [69–71]).

Example 2. Consider bosonic dephasing with local generators $\hat{h}_i = \hat{n}_i$, where $\hat{n}_i$ is the occupation operator of the ith mode. Define the average occupation operator $\hat{n}_{\mathrm{avg}} = \sum_{i=1}^{K} \hat{n}_i/K$, and assume the following constraint on occupation (e.g., energy) fluctuations, $\langle\hat{n}_i\hat{n}_j\rangle - \langle\hat{n}_i\rangle\langle\hat{n}_j\rangle \leq \bar{n}^2$ where $\bar{n} = \langle\hat{n}_{\mathrm{avg}}\rangle$. For entangled and separable strategies, respectively, we find

$$\mathcal{F}_{\mathcal{Q}}^{\mathrm{ent}}(g) = 4K^2\mathrm{Var}(\hat{n}_{\mathrm{avg}}) \leq 4K^2\bar{n}^2, \tag{9}$$

$$\mathcal{F}_{\mathcal{Q}}^{\mathrm{sep}}(g) = 4K\left(\sum_{i=1}^{K}\mathrm{Var}(\hat{n}_i)/K\right) \leq 4K\bar{n}^2. \tag{10}$$

Up to a small correction $\mathcal{O}(\bar{n} - \lfloor\bar{n}\rfloor)$, the optimal separable probe is the product state $\big((|0\rangle + |N\rangle)/\sqrt{2}\big)^{\otimes K}$, where $N = \lfloor\bar{n}\rfloor$. The optimal entangled probe is the bosonic GHZ state $(|00\ldots0\rangle + |NN\ldots N\rangle)/\sqrt{2}$, which is an entangled non-Gaussian state. In fact, to reach the limit implied by Eq. (9), entangled non-Gaussian states are necessary (see Appendix C for details).

We readily incorporate fermionic dephasing [78, 79], which shares similarities to spin dephasing [Eqs. (7) and (8)] and bosonic dephasing [Eqs. (9) and (10)]. Analogous to the bosonic case, $\hat{n}_i$ denotes the fermionic occupation operator responsible for dephasing on the ith fermionic mode. However, due to the Pauli exclusion principle, the fermionic occupation per mode is restricted to $N = 1$. For an even number of modes, the optimal probe is the fermionic GHZ state.

Example 3. Consider random bosonic displacements with local generators $\hat{h}_i = \hat{p}_i$, where $\hat{p}_i$ is the momentum operator at the ith sensor. Define the average momentum operator $\hat{p}_{\mathrm{avg}} = \sum_{i=1}^{K} \hat{p}_i/K$, and assume a total occupation constraint, $\sum_{i=1}^{K}\langle\hat{n}_i\rangle \leq K\bar{n}$, for any input probe state. For entangled and separable strategies, respectively, we find

$$\mathcal{F}_{\mathcal{Q}}^{\mathrm{ent}}(g) = 4K^2\mathrm{Var}(\hat{p}_{\mathrm{avg}}) \leq 8K^2(\bar{n} + 1/2), \tag{11}$$

$$\mathcal{F}_{\mathcal{Q}}^{\mathrm{sep}}(g) = 4K\left(\sum_{i=1}^{K}\mathrm{Var}(\hat{p}_i)/K\right) \leq 8K(\bar{n} + 1/2). \tag{12}$$

The optimal separable probe is a product of K squeezed vacuum states, each with $\bar{n}$ quanta [80]. The optimal entangled probe is a distributed squeezed vacuum state (see Ref. [24]) of $K\bar{n}$ quanta. References [59, 62] explored this estimation problem with QSNs consisting of microwave resonators and opto-mechanical sensors but did not discuss ultimate limits nor schemes to approach them (though see Supplementary Note 6 of Ref. [43]).

Sensing protocol.—Equation (4) [and by extension, Eq. (5)] allows us to establish fundamental precision limits on correlated noise estimation problems. However, another challenge lies in designing measurements and estimation strategies that achieve such limits. In multiparameter settings [as indicated via Eq. (4)], the saturability of such limits is generally uncertain [75]. Whereas, for single parameter estimation, maximum likelihood estimation achieves the QFI [73, 74]. Remarkably, for the class of single-parameter problems considered here, i.e.,

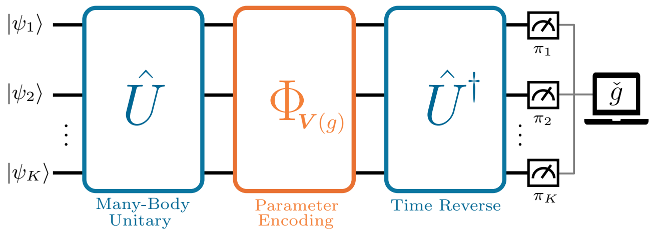

FIG. 1. QSN Echo Protocol. Generate multi-sensor entangled probe, $|\psi\rangle$, by acting with many-body unitary, $\hat{U}$, on local sensor states, $\{|\psi_i\rangle\}$. Quantum channel $\Phi_{\boldsymbol{V}}$ encodes parameter g into probe. Revert the many-body unitary via $\hat{U}^\dagger$. Perform local projective measurements, $\pi_i = |\psi_i\rangle\langle\psi_i|$, and estimate g from the measurement statistics.

$\boldsymbol{V} = g^2\boldsymbol{v}$ and $\mathrm{Tr}\{g^2\boldsymbol{v}\boldsymbol{\mathcal{H}}\} \ll 1$, there exists an explicit, universally optimal measurement protocol, which consists of projecting the output of the channel onto the input state (cf. [42, 81]). We elaborate further below.

Consider the entangled probe $\rho = |\psi\rangle\langle\psi|$, and define the measurements $M_0 = |\psi\rangle\langle\psi|$ and $M_1 = I - M_0$. Using Eq. (1), we directly calculate the measurement probabilities: $p_0 = \mathrm{Tr}\{M_0\Phi_{\boldsymbol{V}}(|\psi\rangle\langle\psi|)\} \approx 1 - g^2\,\mathrm{Tr}\{\boldsymbol{v}\boldsymbol{\mathcal{H}}\}$ and $p_1 \approx g^2\,\mathrm{Tr}\{\boldsymbol{v}\boldsymbol{\mathcal{H}}\}$. From here, we compute the classical Fisher information for this measurement procedure, $\mathcal{F}_{\mathcal{C}}(g) = \sum_{i=0}^{1}(\partial_g p_i)^2/p_i \approx 4\,\mathrm{Tr}\{\boldsymbol{v}\boldsymbol{\mathcal{H}}\}$, which achieves the QFI in Eq. (5). Notably, this procedure does not depend on problem specifics nor the physical systems involved, whether they be qubits, fermions, or bosons.

The measurement protocol above resembles an (Loschmidt) echo sequence [82, 83] (cf. [37, 66]). See Fig. 1 for an illustration. Suppose we prepare the probe, ψ, by acting with the unitary circuit U on local quantum states, ψ_i, such that $|\psi\rangle = U\big(\bigotimes_{i=1}^{K}|\psi_i\rangle\big)$. Then, we interpret the protocol as the following sequence: (1) Prepare the sensors in local product states, $\bigotimes_{i=1}^{K}|\psi_i\rangle$. (2) Entangle the sensors with the many-body operation $\hat{U}$. (3) Encode parameter g via $\Phi_{\boldsymbol{V}}$. (4) Evolve the sensors under $U^\dagger$, i.e., the time-reverse of U. (5) Perform local projective measurements, $\pi_i = |\psi_i\rangle\langle\psi_i|$, and construct the binary POVM $\{M_0, I - M_0\}$, with $M_0 = \bigotimes_i \pi_i$, to estimate g from the measurement data.

Multiple noise parameters.—The case of multiple unknown parameters [75] poses significant challenges compared to the single-parameter examples discussed thus far. We observed entanglement advantage when estimating the single noise parameter g [i.e., case (i)] and elaborated on achievability with specific sensing protocols. It is interesting to consider whether or not an advantage also appears in multi-parameter problems. We argue that an entanglement advantage is conceivable if we restrict ourselves to estimating $n < K$ non-local, aggregate parameters [23, 26, 72]. The advantage disappears at $n = K$ and reduces to that of our aforementioned single-parameter protocol at $n = 1$, interpolating between the two extreme cases.

We construct the following multi-parameter example, which falls under case (ii). Consider the (user-specified) orthogonal matrix $\boldsymbol{W} = (\vec{w}_1, \ldots, \vec{w}_K)^\top$, such that $\vec{w}_I^\top\vec{w}_J = \delta_{IJ}$. Let $\boldsymbol{V}'_{IJ} \coloneqq \vec{w}_I^\top\boldsymbol{V}\vec{w}_J$, and parametrize $\boldsymbol{V}'$ via $\boldsymbol{V}'_{IJ} = \xi_I\xi_J\mathscr{C}_{IJ}$, where $\xi_I^2 \coloneqq \vec{w}_I^\top\boldsymbol{V}\vec{w}_I$. Here, $\mathscr{C}_{II} = 1$ and $\mathscr{C}_{IJ} \le 1$ otherwise [84], and we assume no knowledge of the elements of $\boldsymbol{V}$. We are interested in estimating aggregate parameters $\Xi \coloneqq \{\xi_I\}_{I=1}^{K}$, which describe fluctuations of the Ith non-local, collective mode. The numbers $\mathscr{C}_{IJ}$ $(I \neq J)$ represent correlation coefficients, which we treat as nuisance parameters here. We state the following claim, which we prove in Appendix D.

Claim. *The diagonal elements of the QFI matrix for the parameter set of non-local fluctuation* Ξ *are*

$$(\boldsymbol{\mathcal{F}}_{\mathcal{Q}}(\Xi))_{II} = 4\vec{w}_I^\top\boldsymbol{\mathcal{H}}\vec{w}_I. \tag{13}$$

Equation (13) suggests a simultaneous entanglement advantage in estimating all parameters in Ξ. However, the QFI bounds the error from below [see Eq. (2)], and the corresponding bound is, generically, not saturable for multiple parameters [75]. Though, if only the subset of parameters $\Xi_n \subset \Xi$, with $n < K$, interest us, it then seems plausible to achieve a *simultaneous* entanglement advantage ($\propto K/n$) over separable probes $\forall\,\xi_I \in \Xi_n$. We support this conjecture through an example involving random bosonic displacements, e.g., correlated quadrature fluctuations in a system of K oscillators.

Consider the random displacement channel $\Phi_{\boldsymbol{V}}$, where $\boldsymbol{V}$ denotes the $(K \times K)$ covariance of displacements generated by local momenta $\{\hat{p}_i\}_{i=1}^{K}$. Let $\boldsymbol{V}'_{IJ} = \vec{w}_I^\top\boldsymbol{V}\vec{w}_J$ represent non-local fluctuations generated by collective momenta $\{\hat{P}_I\}_{I=1}^{K}$, where $\hat{P}_I = \sum_i(\vec{w}_I)_i\hat{p}_i$. In other words, $\boldsymbol{V}'_{II} \eqqcolon \xi_I^2$ symbolizes displacement fluctuations along the Ith collective mode of the QSN. Equation (13) then implies that $\mathcal{F}^{\mathrm{ent}}(\xi_I) \propto \mathrm{Var}(\hat{P}_I)$, while for separable strategies, $\mathcal{F}^{\mathrm{sep}}(\xi_I) \propto \sum_{i=1}^{K}\boldsymbol{W}_{Ii}^2\mathrm{Var}(\hat{p}_i)$. We direct our attention to simultaneously estimating all parameters in the the subset $\Xi_n = \{\xi_I\}_{I=1}^{n}$ with $n < K$, for a fixed total occupation, $K\bar{n}$. For the entangled strategy, we must only populate (e.g., squeeze) the n collective modes—thus forming a continuous-variable entangled state of the QSN—with $\mathrm{Var}(\hat{P}_I) \approx K\bar{n}/n$ for every $I \in \{1, \ldots, n\}$ [64]. Contrariwise, the separable strategy requires populating all K local sensor modes with $\bar{n}$ quanta each. It follows that $\mathcal{F}^{\mathrm{ent}}/\mathcal{F}^{\mathrm{sep}} \propto K/n$, suggesting a simultaneous entanglement advantage over separable strategies for *every* parameter $\xi_I \in \Xi_n$.

A variant of the echo sensing protocol realizes the above advantage [85]. This resembles the original distributed sensing scheme of Refs. [24, 64] but, crucially, employs anti-squeezing and photon counting (rather than homodyne detection) at the measurement end.

Discussion.—We have investigated entanglement advantage when estimating collective stochastic properties with QSNs. In doing so, we have shown how quantum correlations within the QSN *and* classical (spatial) correlations within the noise process must collude to enable an entanglement advantage. The classical correlations are paramount, since entanglement alone does not improve the estimation of independent noises [38, 77]. Intuitively, this is because the noise impacts a collective mode of the QSN (e.g., the center-of-mass quadrature, collective spin etc.), rather than impacting the local sensor modes independently. As a result, a many-body quantum state, sensitive to fluctuations of one or more collective modes, improves estimation of the non-local noise process.

It is instructive to compare our correlated noise estimation protocols to conventional unitary estimation. In unitary estimation, having K copies of the unitary channel $\hat{U}^{\otimes K}$ (e.g., with global Hamiltonian $\hat{H} = \vartheta \sum_{i=1}^{K} \hat{h}_i$) and entanglement between the K sensors improves estimation, resulting in Heisenberg scaling with K [2]. In contrast, having K copies of a single-sensor noise channel φ, $\varphi^{\otimes K}$, typically results in shot-noise scaling with K [49, 51]. Albeit, as we have shown, given a single copy of the K-sensor noise channel Φ, classical (spatial) correlations within the channel (i.e., such that $\Phi \neq \varphi^{\otimes K}$), enables Heisenberg scaling via entanglement in the QSN.

Another distinction lies in environmental effects. In unitary estimation, decoherence generated by the same Hamiltonian as the unitary process (i.e., parallel decoherence [53]) inhibits Heisenberg scaling [53–55]. Whereas, for correlated noise estimation, we show in Appendix E that an entanglement advantage persists in the face of parallel decoherence (e.g., additive background noise). However, we do observe that parallel decoherence conjures Rayleigh's curse [45, 86]—that is, the QFI vanishes as the signal tends to zero.

We have focused on simple problem setups, leaving room for further investigation in correlated noise estimation. Developing a more comprehensive view of multiparameter problems will be valuable, especially concerning optimal measurement strategies beyond the displacement sensing problem that we address. Assessing what role quantum control has to play in these contexts should prove fruitful [53, 87]. Additionally, evaluating the impact of deleterious decoherence, with distinct generators from the signal, offers meaningful insights. For example, estimating random bosonic displacements in the presence of loss presents challenges, where, in contrast to the lossless case, perfect quantum memories or non-Gaussian probes are required [43, 45, 88]. From a broader physics perspective, applications to searches for new physics with QSNs [57–62] and many-body quantum metrology [67] exemplify compelling avenues for continued exploration.

ACKNOWLEDGMENTS

Acknowledgments.—The authors acknowledge Jacob Bringewatt for meaningful conversations. A.J.B. acknowledges support from the NRC Research Associateship Program at NIST; A.J.B. was supported by ONR N00014-23-1-2296 at USC for the initial part of the work. Y.-X.W. acknowledges support from a QuICS Hartree Postdoctoral Fellowship. Q.Z. acknowledges NSF (CCF-2240641,OMA-2326746,2350153), ONR N00014-23-1-2296, AFOSR MURI FA9550-24-1-0349 and DARPA (HR00112490362,HR00112490453,HR001123S0052). A.V.G. was supported in part by AFOSR MURI, DARPA SAVaNT ADVENT, NSF QLCI (award No. OMA-2120757), NSF STAQ program, DoE ASCR Accelerated Research in Quantum Computing program (awards No. DE-SC0020312 and No. DE-SC0025341), and DoE ASCR Quantum Testbed Pathfinder program (awards No. DE-SC0019040 and No. DE-SC0024220). A.V.G. also acknowledges support from the U.S. Department of Energy, Office of Science, National Quantum Information Science Research Centers, Quantum Systems Accelerator.

[1] V. Giovannetti, S. Lloyd, and L. Maccone, Quantum-Enhanced Measurements: Beating the Standard Quantum Limit, Science **306**, 1330 (2004).
[2] V. Giovannetti, S. Lloyd, and L. Maccone, Quantum Metrology, Phys. Rev. Lett. **96**, 010401 (2006).
[3] C. L. Degen, F. Reinhard, and P. Cappellaro, Quantum sensing, Rev. Mod. Phys. **89**, 035002 (2017).
[4] V. Bužek, R. Derka, and S. Massar, Optimal Quantum Clocks, Phys. Rev. Lett. **82**, 2207 (1999).
[5] A. D. Ludlow, M. M. Boyd, J. Ye, E. Peik, and P. O. Schmidt, Optical atomic clocks, Rev. Mod. Phys. **87**, 637 (2015).
[6] L. Pezzè, A. Smerzi, M. K. Oberthaler, R. Schmied, and P. Treutlein, Quantum metrology with nonclassical states of atomic ensembles, Rev. Mod. Phys. **90**, 035005 (2018).
[7] J. M. Robinson, M. Miklos, Y. M. Tso, C. J. Kennedy, T. Bothwell, D. Kedar, J. K. Thompson, and J. Ye, Direct comparison of two spin-squeezed optical clock ensembles at the 10^{-17} level, Nat. Phys. **20**, 208 (2024).
[8] M. J. Holland and K. Burnett, Interferometric detection of optical phase shifts at the Heisenberg limit, Phys. Rev. Lett. **71**, 1355 (1993).
[9] T. Nagata, R. Okamoto, J. L. O'Brien, K. Sasaki, and S. Takeuchi, Beating the Standard Quantum Limit with Four-Entangled Photons, Science **316**, 726 (2007).
[10] W. Wang, Y. Wu, Y. Ma, W. Cai, L. Hu, X. Mu, Y. Xu, Z.-J. Chen, H. Wang, Y. Song, *et al.*, Heisenberg-limited single-mode quantum metrology in a superconducting circuit, Nat. Commun. **10**, 4382 (2019).
[11] X. Deng, S. Li, Z.-J. Chen, Z. Ni, Y. Cai, J. Mai, L. Zhang, P. Zheng, H. Yu, C.-L. Zou, *et al.*, Quantum-enhanced metrology with large Fock states, Nat. Phys. , 1 (2024).
[12] F. Wolf, C. Shi, J. C. Heip, M. Gessner, L. Pezzè, A. Smerzi, M. Schulte, K. Hammerer, and P. O. Schmidt, Motional Fock states for quantum-enhanced amplitude

and phase measurements with trapped ions, Nat. Commun. **10**, 2929 (2019).

[13] K. C. McCormick, J. Keller, S. C. Burd, D. J. Wineland, A. C. Wilson, and D. Leibfried, Quantum-enhanced sensing of a single-ion mechanical oscillator, Nature **572**, 86 (2019).

[14] C. M. Caves, Quantum-mechanical noise in an interferometer, Phys. Rev. D **23**, 1693 (1981).

[15] R. Schnabel, N. Mavalvala, D. E. McClelland, and P. K. Lam, Quantum metrology for gravitational wave astronomy, Nat. Commun. **1**, 121 (2010).

[16] W. Jia, V. Xu, K. Kuns, M. Nakano, L. Barsotti, M. Evans, N. Mavalvala, and members of the LIGO Scientific Collaboration, Squeezing the quantum noise of a gravitational-wave detector below the standard quantum limit, Science **385**, 1318 (2024).

[17] H.-Y. Huang, Y. Tong, D. Fang, and Y. Su, Learning Many-Body Hamiltonians with Heisenberg-Limited Scaling, Phys. Rev. Lett. **130**, 200403 (2023).

[18] H. Li, Y. Tong, T. Gefen, H. Ni, and L. Ying, Heisenberg-limited Hamiltonian learning for interacting bosons, npj Quantum Inf. **10**, 83 (2024).

[19] M. Ma, S. T. Flammia, J. Preskill, and Y. Tong, Learning k-body Hamiltonians via compressed sensing (2024), arXiv:2410.18928 [quant-ph].

[20] A. Mirani and P. Hayden, Learning interacting fermionic Hamiltonians at the Heisenberg limit (2024), arXiv:2403.00069 [quant-ph].

[21] Z. Eldredge, M. Foss-Feig, J. A. Gross, S. L. Rolston, and A. V. Gorshkov, Optimal and secure measurement protocols for quantum sensor networks, Phys. Rev. A **97**, 042337 (2018).

[22] T. J. Proctor, P. A. Knott, and J. A. Dunningham, Networked quantum sensing (2017), arXiv:1702.04271 [quant-ph].

[23] T. J. Proctor, P. A. Knott, and J. A. Dunningham, Multiparameter Estimation in Networked Quantum Sensors, Phys. Rev. Lett. **120**, 080501 (2018).

[24] Q. Zhuang, Z. Zhang, and J. H. Shapiro, Distributed quantum sensing using continuous-variable multipartite entanglement, Phys. Rev. A **97**, 032329 (2018).

[25] W. Ge, K. Jacobs, Z. Eldredge, A. V. Gorshkov, and M. Foss-Feig, Distributed Quantum Metrology with Linear Networks and Separable Inputs, Phys. Rev. Lett. **121**, 043604 (2018).

[26] K. Qian, Z. Eldredge, W. Ge, G. Pagano, C. Monroe, J. V. Porto, and A. V. Gorshkov, Heisenberg-scaling measurement protocol for analytic functions with quantum sensor networks, Phys. Rev. A **100**, 042304 (2019).

[27] T. Qian, J. Bringewatt, I. Boettcher, P. Bienias, and A. V. Gorshkov, Optimal measurement of field properties with quantum sensor networks, Phys. Rev. A **103**, L030601 (2021).

[28] Z. Zhang and Q. Zhuang, Distributed quantum sensing, Quantum Sci. Technol. **6**, 043001 (2021).

[29] P. Komar, E. M. Kessler, M. Bishof, L. Jiang, A. S. Sørensen, J. Ye, and M. D. Lukin, A quantum network of clocks, Nat. Phys. **10**, 582 (2014).

[30] E. M. Kessler, P. Kómár, M. Bishof, L. Jiang, A. S. Sørensen, J. Ye, and M. D. Lukin, Heisenberg-Limited Atom Clocks Based on Entangled Qubits, Phys. Rev. Lett. **112**, 190403 (2014).

[31] B. C. Nichol, R. Srinivas, D. Nadlinger, P. Drmota, D. Main, G. Araneda, C. Ballance, and D. Lucas, An elementary quantum network of entangled optical atomic clocks, Nature **609**, 689 (2022).

[32] B. K. Malia, Y. Wu, J. Martínez-Rincón, and M. A. Kasevich, Distributed quantum sensing with mode-entangled spin-squeezed atomic states, Nature **612**, 661 (2022).

[33] X. Guo, C. R. Breum, J. Borregaard, S. Izumi, M. V. Larsen, T. Gehring, M. Christandl, J. S. Neergaard-Nielsen, and U. L. Andersen, Distributed quantum sensing in a continuous-variable entangled network, Nat. Phys. **16**, 281 (2020).

[34] L.-Z. Liu, Y.-Z. Zhang, Z.-D. Li, R. Zhang, X.-F. Yin, Y.-Y. Fei, L. Li, N.-L. Liu, F. Xu, Y.-A. Chen, *et al.*, Distributed quantum phase estimation with entangled photons, Nat. Photon. **15**, 137 (2021).

[35] Y. Xia, W. Li, W. Clark, D. Hart, Q. Zhuang, and Z. Zhang, Demonstration of a Reconfigurable Entangled Radio-Frequency Photonic Sensor Network, Phys. Rev. Lett. **124**, 150502 (2020).

[36] Y. Xia, A. R. Agrawal, C. M. Pluchar, A. J. Brady, Z. Liu, Q. Zhuang, D. J. Wilson, and Z. Zhang, Entanglement-enhanced optomechanical sensing, Nat. Photon. **17**, 470 (2023).

[37] K. A. Gilmore, M. Affolter, R. J. Lewis-Swan, D. Barberena, E. Jordan, A. M. Rey, and J. J. Bollinger, Quantum-enhanced sensing of displacements and electric fields with two-dimensional trapped-ion crystals, Science **373**, 673 (2021).

[38] J. Kołodyński and R. Demkowicz-Dobrzański, Efficient tools for quantum metrology with uncorrelated noise, New J. Phys. **15**, 073043 (2013).

[39] S. Pirandola and C. Lupo, Ultimate Precision of Adaptive Noise Estimation, Phys. Rev. Lett. **118**, 100502 (2017).

[40] Z. Huang, L. Lami, and M. M. Wilde, Exact Quantum Sensing Limits for Bosonic Dephasing Channels, PRX Quantum **5**, 020354 (2024).

[41] S. Ng, S. Z. Ang, T. A. Wheatley, H. Yonezawa, A. Furusawa, E. H. Huntington, and M. Tsang, Spectrum analysis with quantum dynamical systems, Phys. Rev. A **93**, 042121 (2016).

[42] W. Górecki, A. Riccardi, and L. Maccone, Quantum Metrology of Noisy Spreading Channels, Phys. Rev. Lett. **129**, 240503 (2022).

[43] H. Shi and Q. Zhuang, Ultimate precision limit of noise sensing and dark matter search, npj Quantum Inf. **9**, 27 (2023).

[44] M. Tsang, Quantum noise spectroscopy as an incoherent imaging problem, Phys. Rev. A **107**, 012611 (2023).

[45] J. W. Gardner, T. Gefen, S. A. Haine, J. J. Hope, J. Preskill, Y. Chen, and L. McCuller, Stochastic waveform estimation at the fundamental quantum limit (2024), arXiv:2404.13867 [quant-ph].

[46] W. Górecki, F. Albarelli, S. Felicetti, R. D. Candia, and L. Maccone, Interplay between time and energy in bosonic noisy quantum metrology (2024), arXiv:2409.18791 [quant-ph].

[47] S. T. Flammia and J. J. Wallman, Efficient Estimation of Pauli Channels, ACM Trans. Quantum Comp. **1**, 1–32 (2020).

[48] R. Harper, S. T. Flammia, and J. J. Wallman, Efficient learning of quantum noise, Nat. Phys. **16**, 1184 (2020).

[49] Z. Ji, G. Wang, R. Duan, Y. Feng, and M. Ying, Parameter Estimation of Quantum Channels, IEEE Trans. Inf. Theory **54**, 5172–5185 (2008).

[50] B. M. Escher, R. L. de Matos Filho, and L. Davidovich, General framework for estimating the ultimate precision limit in noisy quantum-enhanced metrology, Nat. Phys. **7**, 406–411 (2011).

[51] R. Demkowicz-Dobrzański, J. Kołodyński, and M. Guţă, The elusive Heisenberg limit in quantum-enhanced metrology, Nat. Commun. **3**, 1063 (2012).

[52] R. Demkowicz-Dobrzański and L. Maccone, Using Entanglement Against Noise in Quantum Metrology, Phys. Rev. Lett. **113**, 250801 (2014).

[53] P. Sekatski, M. Skotiniotis, J. Kołodyński, and W. Dür, Quantum metrology with full and fast quantum control, Quantum **1**, 27 (2017).

[54] R. Demkowicz-Dobrzański, J. Czajkowski, and P. Sekatski, Adaptive Quantum Metrology under General Markovian Noise, Phys. Rev. X **7**, 041009 (2017).

[55] S. Zhou, M. Zhang, J. Preskill, and L. Jiang, Achieving the Heisenberg limit in quantum metrology using quantum error correction, Nat. Commun. **9**, 78 (2018).

[56] J. Jeske, J. H. Cole, and S. F. Huelga, Quantum metrology subject to spatially correlated Markovian noise: restoring the Heisenberg limit, New J. Phys. **16**, 073039 (2014).

[57] J. Ye and P. Zoller, Essay: Quantum Sensing with Atomic, Molecular, and Optical Platforms for Fundamental Physics, Phys. Rev. Lett. **132**, 190001 (2024).

[58] S. D. Bass and M. Doser, Quantum sensing for particle physics, Nat. Rev. Phys. **6**, 329–339 (2024).

[59] A. J. Brady, C. Gao, R. Harnik, Z. Liu, Z. Zhang, and Q. Zhuang, Entangled Sensor-Networks for Dark-Matter Searches, PRX Quantum **3**, 030333 (2022).

[60] S. Chen, H. Fukuda, T. Inada, T. Moroi, T. Nitta, and T. Sichanugrist, Quantum Enhancement in Dark Matter Detection with Quantum Computation, Phys. Rev. Lett. **133**, 021801 (2024).

[61] A. Ito, R. Kitano, W. Nakano, and R. Takai, Quantum entanglement of ions for light dark matter detection, J. High Energ. Phys. **2024** (2), 1.

[62] A. J. Brady, X. Chen, Y. Xia, J. Manley, M. Dey Chowdhury, K. Xiao, Z. Liu, R. Harnik, D. J. Wilson, Z. Zhang, *et al.*, Entanglement-enhanced optomechanical sensor array with application to dark matter searches, Commun. Phys. **6**, 237 (2023).

[63] W. Ji, Z. Liu, Y. Guo, Z. Hu, J. Zhou, S. Dai, Y. Chen, P. Yu, M. Wang, K. Xia, *et al.*, Correlated sensing with a solid-state quantum multisensor system for atomic-scale structural analysis, Nat. Photon. **18**, 230 (2024).

[64] Q. Zhuang and Z. Zhang, Physical-Layer Supervised Learning Assisted by an Entangled Sensor Network, Phys. Rev. X **9**, 041023 (2019).

[65] Y. Xia, W. Li, Q. Zhuang, and Z. Zhang, Quantum-Enhanced Data Classification with a Variational Entangled Sensor Network, Phys. Rev. X **11**, 021047 (2021).

[66] S. Colombo, E. Pedrozo-Penafiel, A. F. Adiyatullin, Z. Li, E. Mendez, C. Shu, and V. Vuletić, Time-reversal-based quantum metrology with many-body entangled states, Nat. Phys. **18**, 925 (2022).

[67] V. Montenegro, C. Mukhopadhyay, R. Yousefjani, S. Sarkar, U. Mishra, M. G. A. Paris, and A. Bayat, Review: Quantum Metrology and Sensing with Many-Body Systems (2024), arXiv:2408.15323 [quant-ph].

[68] H. Hainzer, D. Kiesenhofer, T. Ollikainen, M. Bock, F. Kranzl, M. K. Joshi, G. Yoeli, R. Blatt, T. Gefen, and C. F. Roos, Correlation Spectroscopy with Multiqubit-Enhanced Phase Estimation, Phys. Rev. X **14**, 011033 (2024).

[69] Y. Matsuzaki, S. Saito, and W. J. Munro, Quantum metrology at the Heisenberg limit with the presence of independent dephasing (2018), arXiv:1809.00176 [quant-ph].

[70] Y.-X. Wang, J. Bringewatt, A. Seif, A. J. Brady, C. Oh, and A. V. Gorshkov, Exponential entanglement advantage in sensing correlated noise (2024), arXiv:2410.05878 [quant-ph].

[71] A. Dey, S. Mouradian, C. Lupo, and Z. Huang, Quantum-Optimal Frequency Estimation of Stochastic AC Fields (2024), arXiv:2411.19412 [quant-ph].

[72] J. Bringewatt, I. Boettcher, P. Niroula, P. Bienias, and A. V. Gorshkov, Protocols for estimating multiple functions with quantum sensor networks: Geometry and performance, Phys. Rev. Res. **3**, 033011 (2021).

[73] M. G. A. Paris, Quantum estimation for quantum technology, Int. J. Quantum Inf. **7**, 125 (2009).

[74] J. S. Sidhu and P. Kok, Geometric perspective on quantum parameter estimation, AVS Quantum Sci. **2**, 014701 (2020).

[75] J. Liu, H. Yuan, X.-M. Lu, and X. Wang, Quantum Fisher information matrix and multiparameter estimation, J. Phys. A: Math. Theor. **53**, 023001 (2020).

[76] S. L. Braunstein and C. M. Caves, Statistical distance and the geometry of quantum states, Phys. Rev. Lett. **72**, 3439 (1994).

[77] M. Hotta, T. Karasawa, and M. Ozawa, N-body-extended channel estimation for low-noise parameters, J. Phys. A: Math. Gen. **39**, 14465 (2006).

[78] D. González-Cuadra, D. Bluvstein, M. Kalinowski, R. Kaubruegger, N. Maskara, P. Naldesi, T. V. Zache, A. M. Kaufman, M. D. Lukin, H. Pichler, *et al.*, Fermionic quantum processing with programmable neutral atom arrays, Proc. Natl. Acad. Sci. **120**, e2304294120 (2023).

[79] A. Schuckert, E. Crane, A. V. Gorshkov, M. Hafezi, and M. J. Gullans, Fermion-qubit fault-tolerant quantum computing (2024), arXiv:2411.08955 [quant-ph].

[80] A Fock state is 3dB shy of the QFI. This stems from the fact that estimating random single-quadrature displacements differs slightly from estimating displacements on both quadratures, e.g., position and momentum fluctuations. For the latter, both Fock states and squeezed vacuum states are optimal in the lossless regime [12, 42].

[81] T. Gefen, A. Rotem, and A. Retzker, Overcoming resolution limits with quantum sensing, Nat. Commun. **10**, 4992 (2019).

[82] T. Macrì, A. Smerzi, and L. Pezzè, Loschmidt echo for quantum metrology, Phys. Rev. A **94**, 010102 (2016).

[83] C. Yin, V. V. Albert, and S. Zhou, Small correlation is sufficient for optimal noisy quantum metrology (2024), arXiv:2408.00079 [quant-ph].

[84] There are also negativity conditions on $\mathscr{C}_{IJ}$, set by $\boldsymbol{V}' > 0$, which is unimportant to our discussion.

[85] The variation of the echo protocol comes in the final measurement step, which now involves n independent POVMs, $\bigoplus_{I=1}^{n}\{M_0^{(I)}, I - M_0^{(I)}\}$ used to simultaneously estimate each $\xi_I \in \Xi_n$. For (distributed) squeezed vacuum inputs, the measurements consist of anti-squeezing followed by photon counting [42–44].

[86] M. Tsang, R. Nair, and X.-M. Lu, Quantum Theory of Superresolution for Two Incoherent Optical Point Sources, Phys. Rev. X **6**, 031033 (2016).

[87] J. Bringewatt, A. Ehrenberg, T. Goel, and A. V. Gorshkov, Optimal function estimation with photonic quantum sensor networks, Phys. Rev. Res. **6**, 013246 (2024).

[88] H. Shi, A. J. Brady, W. Górecki, L. Maccone, R. D. Candia, and Q. Zhuang, Quantum-enhanced dark matter detection with in-cavity control: mitigating the Rayleigh curse (2024), arXiv:2409.04656 [quant-ph].

[89] D. Manzano, A short introduction to the Lindblad master equation, AIP Advances **10**, 025106 (2020).

[90] A. Serafini, *Quantum Continuous Variables: A Primer of Theoretical Methods* (CRC Press, 2017).

APPENDICES

Here we provide details otherwise omitted in the main text. In Section A, we motivate the form of the approximate quantum channel utilized throughout the article. In Section B, we derive the Result [Eq. (4)] of the main text, i.e. the direct relation between the QFI matrix and the (weak) noise covariance $\boldsymbol{V}$ of the quantum channel $\Phi_{\boldsymbol{V}}$. In Section C, we derive a no-go result for entanglement enhanced dephasing estimation with entangled states generated by (passive) linear optics. In Section D, we derive the QFI matrix for multiple noise parameters (see Claim [Eq. (13)] of main text). In Section E, we elaborate on how parallel decoherence triggers Rayleigh's curse in noise estimation problems.

Appendix A: Details About Approximate Noise Channel

In this section, we motivate the form of the approximate quantum channel [Eq. (1)] analyzed throughout the main text. Recall the approximate form of the QSN noise channel $\Phi_{\boldsymbol{V}}$, which we write out here for convenience,

$$\Phi_{\boldsymbol{V}}(\rho) \approx \rho + \sum_{i,j=1}^{K} \boldsymbol{V}_{ij} \left(\hat{h}_i \rho \hat{h}_j - \frac{1}{2} \left\{ \hat{h}_i \hat{h}_j, \rho \right\} \right). \tag{A1}$$

We consider two physical, yet fairly generic, settings where this approximation applies: (a) short time open-system dynamics and (b) weak, random unitary channels. The explicit examples of spin dephasing, bosonic (fermionic) dephasing, and bosonic random displacements considered in the article fall within either setting.

a. Short Time Open-System Dynamics. The expansion (A1) mimics open-system dynamics described through the Lindblad master equation [89]. To reveal the correspondence, we first write the (Markovian) master equation in its general form,

$$\partial_t \rho = -i[\hat{H}_S, \rho] + \sum_{i,j} \boldsymbol{\gamma}_{ij} \left(\hat{A}_j \rho \hat{A}_i^\dagger - \frac{1}{2} \left\{ \hat{A}_i^\dagger \hat{A}_j, \rho \right\} \right), \tag{A2}$$

where $\hat{H}_S$ is the system Hamiltonian, $\boldsymbol{\gamma}$ is the positive semi-definite matrix symbolizing the system's decoherence processes (per unit time), and $\{\hat{A}_j\}$ are jump operators. For purely noisy dynamics, as considered here, we take $\hat{H}_S = 0$. Further, suppose the jump operators are Hermitian, i.e. $\hat{A}_i^\dagger = \hat{A}_i$, though this may be generalized. Consider an infinitesimal time interval Δt, such that $\partial_t \rho \approx (\rho(t + \Delta t) - \rho(t))/\Delta t$. We then make the following correspondences, $\Phi_{\boldsymbol{V}}(\rho) = \rho(t + \Delta t)$, $\hat{h}_i = \hat{A}_i$, and $\boldsymbol{V}_{ij} = \boldsymbol{\gamma}_{ij} \Delta t$. Hence, estimation problems associated with $\boldsymbol{V}$ equate to estimation problems associated with the decoherences $\boldsymbol{\gamma}$ over the short time Δt.

b. Weak, Random Unitary Channels. Consider the set of hermitian generators $\vec{\hat{h}} = (\hat{h}_1, \hat{h}_2, \ldots, \hat{h}_K)$ which induce shifts $\vec{\lambda} = (\lambda_1, \lambda_2, \ldots, \lambda_K)$ on a quantum system described by the state ρ. For simplicity, we assume the generators are independent of $\vec{\lambda}$, while the λ_j's are stochastic and described by the probability distribution, $p(\vec{\lambda})$. We associate a single realization of shifts with the parametrized unitary,

$$\hat{U}_{\vec{\lambda}} = e^{-i\vec{\lambda}^\top \vec{\hat{h}}}. \tag{A3}$$

The following quantum channel describes the (random) evolution of the quantum system,

$$\Phi(\rho) = \int \mathrm{d}\vec{\lambda}\, p(\vec{\lambda}) \hat{U}_{\vec{\lambda}} \rho \hat{U}_{\vec{\lambda}}^\dagger, \tag{A4}$$

Herein, we focus on dynamics associated with the mean $\vec{\mu} = \mathbb{E}[\vec{\lambda}]$ and covariance matrix $\boldsymbol{V}_{ij} = \mathbb{E}[\Delta\vec{\lambda}_i \Delta\vec{\lambda}_j]$, where $\Delta\vec{\lambda} \coloneqq \vec{\lambda} - \vec{\mu}$. The mean determines the unitary part of the evolution, while $\boldsymbol{V}$ describes fluctuations about the mean. We do not concern ourselves with higher order moments, supposing that fluctuations are weak.

Lemma 1. *Assume fluctuations weakly perturb the quantum system, ρ, and the "energy" of the system is sufficiently small, such that $\mathbb{E}[\Delta\vec{\lambda}_{i_1}\dots\Delta\vec{\lambda}_{i_n}\hat{h}_{i_1}\dots\hat{h}_{i_n}] \sim \varepsilon^n$ for $n \geq 2$ and $\varepsilon \to 0$. If (1) the generators commute to a constant ($[\hat{h}_i, \hat{h}_j] = \boldsymbol{c}_{ij}\hat{I}$) or (2) the channel mean vanishes ($\vec{\mu} = 0$), then,*

$$\Phi_{\boldsymbol{V}}(\rho) \coloneqq \hat{U}_{\vec{\mu}}^\dagger \Phi(\rho) \hat{U}_{\vec{\mu}} \approx \rho + \sum_{i,j} \boldsymbol{V}_{ij} \left(\hat{h}_i \rho \hat{h}_j - \frac{1}{2} \left\{ \hat{h}_i \hat{h}_j, \rho \right\} \right) + \mathcal{O}(\varepsilon^3). \tag{A5}$$

Proof. We adopt Einstein summation convention, i.e. repeated indices are summed over. Further, we assume that fluctuations are sufficiently small and expand to first non-trivial order around the mean, $\mathbb{E}[\vec{\lambda}] = \vec{\mu}$. For brevity, we define the fluctuation $\Delta\vec{\lambda}_j \coloneqq \vec{\lambda}_j - \vec{\mu}_j$, such that $\mathbb{E}[\Delta\vec{\lambda}] = 0$ and $\boldsymbol{V}_{ij} = \mathbb{E}[\Delta\vec{\lambda}_i \Delta\vec{\lambda}_j]$.

Consider the unitary operator from Eq. (A3) and rewrite it as follows:

$$\hat{U}_{\vec{\lambda}} = e^{-i\vec{\lambda}^\top \hat{\vec{h}}} = e^{-i\Delta\vec{\lambda}^\top \hat{\vec{h}} - i\vec{\mu}^\top \hat{\vec{h}}}, \tag{A6}$$

where $\Delta\vec{\lambda} = \vec{\lambda} - \vec{\mu}$. To expand in small fluctuations about the mean, use the Zassenhaus formula,

$$e^{\hat{A}+\hat{B}} = e^{\hat{A}} e^{\hat{B}} e^{-\frac{1}{2}[\hat{A},\hat{B}]} e^{-\frac{1}{6}\left(2[\hat{B},[\hat{A},\hat{B}]] + [\hat{A},[\hat{A},\hat{B}]]\right)} \times \dots, \tag{A7}$$

where ellipsis denote nested commutators of higher order. We attend to case (1) where the commutators between the generators equals a constant. The result for case (2), i.e. zero mean $\vec{\mu} = 0$, presents itself straightforwardly.

Let $[\hat{h}_i, \hat{h}_j] = \boldsymbol{c}_{ij}$, where $\boldsymbol{c}_{ij}^* = -\boldsymbol{c}_{ij}$ are purely imaginary, and take $\hat{A} = -i\vec{\mu}^\top \hat{\vec{h}}$, and $\hat{B} = -i\Delta\vec{\lambda}^\top \hat{\vec{h}}$. Then only the first-order commutator matters and equals $[\hat{A}, \hat{B}] = -\vec{\mu}^\top \boldsymbol{c} \Delta\vec{\lambda}$, which is purely imaginary. We deduce that

$$\hat{U}_{\vec{\lambda}} \rho \hat{U}_{\vec{\lambda}}^\dagger = \hat{U}_{\vec{\mu}} \hat{U}_{\Delta\vec{\lambda}} \rho \hat{U}_{\Delta\vec{\lambda}}^\dagger \hat{U}_{\vec{\mu}}^\dagger. \tag{A8}$$

Expand the fluctuations as

$$\hat{U}_{\Delta\vec{\lambda}} \approx \hat{I} - i\Delta\vec{\lambda}_j \hat{h}_j - \frac{1}{2} \Delta\vec{\lambda}_j \Delta\vec{\lambda}_k \hat{h}_j \hat{h}_k. \tag{A9}$$

The following set of equalities then hold to $\mathcal{O}(\varepsilon^3)$:

$$\begin{aligned}
\Phi(\rho) &= \int \mathrm{d}\vec{\lambda}\, p(\vec{\lambda}) \hat{U}_{\vec{\lambda}} \rho \hat{U}_{\vec{\lambda}}^\dagger && \text{(A10)}\\
&\approx \int \mathrm{d}\vec{\lambda}\, p(\vec{\lambda}) \hat{U}_{\vec{\mu}} \Big(\rho - i\Delta\vec{\lambda}_j \hat{h}_j \rho + i\Delta\vec{\lambda}_j \rho \hat{h}_j + \Delta\vec{\lambda}_j \Delta\vec{\lambda}_k \hat{h}_j \rho \hat{h}_k && \text{(A11)}\\
&\qquad - \frac{1}{2} \Delta\vec{\lambda}_j \Delta\vec{\lambda}_k \hat{h}_j \hat{h}_k \rho - \frac{1}{2} \Delta\vec{\lambda}_j \Delta\vec{\lambda}_k \rho \hat{h}_j \hat{h}_k \Big) \hat{U}_{\vec{\mu}}^\dagger \\
&= \hat{U}_{\vec{\mu}} \left(\rho + \boldsymbol{V}_{jk} \hat{h}_j \rho \hat{h}_k - \frac{1}{2} \boldsymbol{V}_{jk} \rho \hat{h}_j \hat{h}_k - \frac{1}{2} \boldsymbol{V}_{jk} \hat{h}_j \hat{h}_k \rho \right) \hat{U}_{\vec{\mu}}^\dagger, && \text{(A12)}
\end{aligned}$$

which concludes the proof. □

Further comments about the random unitary channel expansion are in order:

- We properly understand the operator expansion in terms of measurement outcomes. Consider measurements $\{M_j\}$ with $\sum_j M_j = I$. Then, $\mathrm{Tr}\{M_j \Delta\lambda^m \hat{h}^m \rho\} \lesssim \varepsilon^m$. For brevity, we have let $\Delta\lambda^m$ and $\hat{h}^m$ denote any mth order product of fluctuations and generators, e.g., $\Delta\lambda^2 \sim \boldsymbol{V}$ and $\hat{h}^2 \sim \hat{h}_i \hat{h}_j$, respectively.

- The analysis above applies to programmable (or classically simulable) channels [49, 51] in the regime of weak noise and finite energy. We note that metrological bounds for programmable channels, as well as more general noise channels [39], typically apply in asymptotic regimes, e.g. infinite-energy, and do not necessarily entail whether entangled probes are necessary to attain the precision limits derived therefrom.

Appendix B: Derivation of the Main Result

In this section, we prove the Result [Eq. (4)] of the main text, which we restate here for convenience: Consider the QSN probe $\rho = |\psi\rangle\langle\psi|$, and let $\boldsymbol{\mathcal{H}}$ denote the "Hamiltonian" generator matrix of ρ, with elements $\boldsymbol{\mathcal{H}}_{ij} = \langle \hat{h}_i \hat{h}_j \rangle - \langle \hat{h}_i \rangle \langle \hat{h}_j \rangle$. Let $\Theta = \{\vartheta_I\}_{I=1}^n$ be the set of unknown parameters that we aim to estimate. We deduce a direct relation between the QFI matrix $\boldsymbol{\mathcal{F}}_{\mathcal{Q}}(\Theta)$, the covariance matrix of the channel $\boldsymbol{V}$, and the generator matrix $\boldsymbol{\mathcal{H}}$:

$$\sum_{I,J=1}^{n} \left(\boldsymbol{\mathcal{F}}_{\mathcal{Q}}(\Theta)\right)_{IJ} \vartheta_I \vartheta_J = 4\,\mathrm{Tr}\{\boldsymbol{V}\boldsymbol{\mathcal{H}}\}. \tag{B1}$$

We note that $\mathrm{Tr}\{\boldsymbol{V}\boldsymbol{\mathcal{H}}\} \sim \mathcal{O}\big(K^2\varepsilon^2\big)$, in accordance with the small parameter ε introduced in Appendix A. To prove the result, we apply the following lemma.

Lemma 2. *Let $\rho_{\boldsymbol{V}} = \Phi_{\boldsymbol{V}}(\rho)$ and assume an input pure state $\rho = |\psi\rangle\langle\psi|$ for the probe. The input-output fidelity of the quantum channel $\Phi_{\boldsymbol{V}}$ is approximately*

$$F(\rho, \rho_{\boldsymbol{V}}) \approx 1 - \mathrm{Tr}\{\boldsymbol{V}\boldsymbol{\mathcal{H}}\}, \tag{B2}$$

where $\boldsymbol{\mathcal{H}}$ is the Hamiltonian covariance matrix in the local basis,

$$\boldsymbol{\mathcal{H}}_{ij} = \langle \hat{h}_i \hat{h}_j \rangle - \langle \hat{h}_i \rangle \langle \hat{h}_j \rangle\,, \tag{B3}$$

with all expectation values evaluated with respect to the pure probe state $\rho = |\psi\rangle\langle\psi|$.

Proof. Recall the approximate form of the quantum channel $\Phi_{\boldsymbol{V}}$ in Eq. (A1). Then, determine the fidelity between the input $\rho = |\psi\rangle\langle\psi|$ and the output $\rho_{\boldsymbol{V}} = \Phi_{\boldsymbol{V}}(|\psi\rangle\langle\psi|)$:

$$\begin{aligned}
F(\rho, \rho_{\boldsymbol{V}}) =& \; \langle\psi|\Phi_{\boldsymbol{V}}\left(|\psi\rangle\langle\psi|\right)|\psi\rangle & \text{(B4)}\\
&\approx \langle\psi|\psi\rangle^2 + \sum_{i,j} \boldsymbol{V}_{ij} \left(\langle\psi|\hat{h}_i(|\psi\rangle\langle\psi|)\hat{h}_j|\psi\rangle - \frac{1}{2}\langle\psi|\Big\{\hat{h}_i\hat{h}_j, |\psi\rangle\langle\psi|\Big\}|\psi\rangle \right) & \text{(B5)}\\
&= 1 + \sum_{i,j} \boldsymbol{V}_{ij} \left(\langle\psi|\hat{h}_i|\psi\rangle \langle\psi|\hat{h}_j|\psi\rangle - \frac{1}{2}\Big(\langle\psi|\hat{h}_i\hat{h}_j|\psi\rangle \langle\psi|\psi\rangle + \langle\psi|\psi\rangle \langle\psi|\hat{h}_i\hat{h}_j|\psi\rangle \Big) \right) & \text{(B6)}\\
&= 1 + \sum_{i,j} \boldsymbol{V}_{ij} \Big(\langle\psi|\hat{h}_i|\psi\rangle \langle\psi|\hat{h}_j|\psi\rangle - \langle\psi|\hat{h}_i\hat{h}_j|\psi\rangle \Big) & \text{(B7)}\\
&= 1 - \sum_{i,j} \boldsymbol{V}_{ij} \Big(\Big\langle \hat{h}_i\hat{h}_j \Big\rangle - \Big\langle \hat{h}_i \Big\rangle \Big\langle \hat{h}_j \Big\rangle \Big) & \text{(B8)}\\
&= 1 - \mathrm{Tr}\{\boldsymbol{\mathcal{H}}\boldsymbol{V}\}, & \text{(B9)}
\end{aligned}$$

where $\langle \hat{O} \rangle = \langle\psi|\hat{O}|\psi\rangle$. □

We now prove the main result.

Proof. Recall the geometric relation between the QFI matrix and the fidelity via Bures distance [75] for any set of parameters $\{\varphi_I\}$, $\sum_{I,J} \left(\boldsymbol{\mathcal{F}}_{\mathcal{Q}}\right)_{IJ} \delta\varphi_I \delta\varphi_J = 8(1 - \sqrt{F(\rho_\varphi, \rho_{\varphi+\delta\varphi})})$, where $F(\rho, \tau) = \mathrm{Tr}[\sqrt{\sqrt{\rho}\tau\sqrt{\rho}}]^2$ is the fidelity. For one state pure, say $\tau = |\psi\rangle\langle\psi|$, the fidelity is simply the overlap, $F(\rho, |\psi\rangle\langle\psi|) = \langle\psi|\rho|\psi\rangle$. In our work, we estimate small (positive) fluctuations ($\vartheta > 0$) from the identity map, so that

$$\sum_{I,J=1}^{n} \left(\boldsymbol{\mathcal{F}}_{\mathcal{Q}}(\Theta)\right)_{IJ} \vartheta_I \vartheta_J = 8(1 - \sqrt{F(\rho_0, \rho_\vartheta)}), \tag{B10}$$

where $\rho_0 = |\psi\rangle\langle\psi|$ and $\rho_\vartheta = \Phi_{\boldsymbol{V}}(\rho_0)$. Using Lemma 2, we find that

$$F(\rho_0, \rho_\vartheta) \approx 1 - \mathrm{Tr}\{\boldsymbol{V}\boldsymbol{\mathcal{H}}\} \implies 1 - \sqrt{F(\rho_0, \rho_\vartheta)} \approx \mathrm{Tr}\{\boldsymbol{V}\boldsymbol{\mathcal{H}}\}/2. \tag{B11}$$

Substituting the latter relation into Eq. (B10), we obtain the result. □

Appendix C: No-Go Entanglement Advantage in Correlated Dephasing Estimation with Entangled States Generated by (Passive) Linear Optics

In this section, we derive a no-go result for entanglement advantage in estimating correlated (bosonic or fermionic) dephasing with entangled states generated by passive linear optics (e.g., entangled Gaussian bosonic states).

Proposition 1. *Entangled probes generated by propagating local, separable probes through a (passive) linear optical network perform no better than separable probes in estimating maximally correlated dephasing.*

Proof. Consider a passive linear-optical network, denoted by the unitary operator $U_{\boldsymbol{B}}$, and a product of single-mode (Gaussian or non-Gaussian) resource states, $|\psi_{\rm sep}\rangle = \bigotimes_{i=1}^{K} |\psi_i\rangle$. Let $|\psi_{\rm ent}\rangle = U_{\boldsymbol{B}} |\psi_{\rm sep}\rangle$ denote the multi-mode entangled state generated by linear optics. Now, define the average photon number operator per mode, $\hat{n}_{\rm avg} := \sum_{i=1}^{K} \hat{n}_i/K$. Recall the QFI for dephasing estimation using entangled and separable strategies, respectively:

$$\mathcal{F}_{\mathcal{Q}}^{\rm ent}(g) = 4K^2 v \mathrm{Var}\left(\hat{n}_{\rm avg}\right), \tag{C1}$$

$$\mathcal{F}_{\mathcal{Q}}^{\rm sep}(g) = 4Kv \left(\sum_{i=1}^{K} \mathrm{Var}(\hat{n}_i)/K \right). \tag{C2}$$

Proving the proposition thus equates to demonstrating that $\mathrm{Var}(\hat{n}_{\rm avg})_{\psi_{\rm ent}} = \mathrm{Var}(\hat{n}_{\rm avg})_{\psi_{\rm sep}} = \sum_{i=1}^{K} \mathrm{Var}(\hat{n}_i)_{\psi_i}/K^2$, where $\mathrm{Var}(\hat{n}_i)_{\psi_i}$ represent the occupation variances of the local states ψ_i. This follows straightforwardly because, for any state $|\varphi\rangle = U_{\boldsymbol{B}} |\phi\rangle$,

$$\begin{aligned}
\mathrm{Var}(\hat{n}_{\rm avg})_{\varphi} &= \langle\varphi|\hat{n}_{\rm avg}^2|\varphi\rangle - \langle\varphi|\hat{n}_{\rm avg}|\varphi\rangle\langle\varphi|\hat{n}_{\rm avg}|\varphi\rangle &\text{(C3)}\\
&= \langle\phi|U_{\boldsymbol{B}}^{\dagger}\hat{n}_{\rm avg}^2 U_{\boldsymbol{B}}|\phi\rangle - \langle\varphi|U_{\boldsymbol{B}}^{\dagger}\hat{n}_{\rm avg}U_{\boldsymbol{B}}|\varphi\rangle\langle\varphi|U_{\boldsymbol{B}}^{\dagger}\hat{n}_{\rm avg}U_{\boldsymbol{B}}|\varphi\rangle &\text{(C4)}\\
&= \langle\phi|\hat{n}_{\rm avg}^2|\phi\rangle - \langle\phi|\hat{n}_{\rm avg}|\phi\rangle\langle\phi|\hat{n}_{\rm avg}|\phi\rangle &\text{(C5)}\\
&= \mathrm{Var}(\hat{n}_{\rm avg})_{\phi}, &\text{(C6)}
\end{aligned}$$

where the penultimate line derives from the fact that $U_{\boldsymbol{B}}$ represents a passive transformation that conserves $\hat{n}_{\rm avg}$. Thus, $\mathrm{Var}(\hat{n}_{\rm avg})_{\psi_{\rm ent}} = \mathrm{Var}(\hat{n}_{\rm avg})_{\psi_{\rm sep}}$, implying that the (separable) product state $|\psi_{\rm sep}\rangle = \bigotimes_i |\psi_i\rangle$, achieves equal performance as the entangled state $|\psi_{\rm ent}\rangle = U_{\boldsymbol{B}} |\psi_{\rm sep}\rangle$. □

Corollary. *Entangled Gaussian bosonic probes perform equally well as separable Gaussian bosonic probes in estimating maximally correlated bosonic dephasing.*

This follows from the fact that we may construct any (multi-mode) entangled Gaussian bosonic state by passing single-mode Gaussian (i.e., squeezed coherent) states through a passive linear optical network [90].

Appendix D: Multiple Noise Parameters

In this section, we derive the QFI matrix [Eq. (13)] for multiple noise parameters; see the Claim in the main text. Consider an invertible transformation matrix $\boldsymbol{W}$, and define the new covariance

$$\boldsymbol{V}' := \boldsymbol{W}\boldsymbol{V}\boldsymbol{W}^{\top}. \tag{D1}$$

Parametrize $\boldsymbol{V}'$ via

$$\boldsymbol{V}' = \begin{pmatrix} \xi_1^2 & \xi_1\xi_2\mathscr{C}_{12} & \dots & \xi_1\xi_K\mathscr{C}_{1K} \\ \xi_1\xi_2\mathscr{C}_{12} & \xi_2^2 & \dots & \xi_2\xi_K\mathscr{C}_{2K} \\ \vdots & \vdots & \ddots & \vdots \\ \xi_1\xi_K\mathscr{C}_{1K} & \xi_2\xi_K\mathscr{C}_{2K} & \dots & \xi_K^2 \end{pmatrix}, \tag{D2}$$

where $\xi_I^2 := \left(\boldsymbol{W}\boldsymbol{V}\boldsymbol{W}^{\top}\right)_{II}$ denote (real) collective fluctuation parameters. The off-diagonal numbers $\mathscr{C}_{IJ}$ are residual correlation coefficients, which we take as nuisance parameters here. We thus focus on estimates of the collective fluctuations $\Xi = \{\xi_I\}_{I=1}^{K}$, for which we find the following [note that $W^{-\top} = (W^{\top})^{-1}$].

Theorem 1. *Consider parametrization $\boldsymbol{V}'$ as in Eq. (D2). The QFI matrix for parameters $\Xi := \{\xi_I\}_{I=1}^K$ is*

$$(\boldsymbol{\mathcal{F}}_Q(\Xi))_{IJ} = \begin{cases} 4(\boldsymbol{W}^{-\top}\boldsymbol{\mathcal{H}}\boldsymbol{W}^{-1})_{II}, & I = J \\ 8\mathscr{C}_{IJ}(\boldsymbol{W}^{-\top}\,\mathrm{Re}\{\boldsymbol{\mathcal{H}}\}\boldsymbol{W}^{-1})_{IJ}, & I \neq J, \end{cases} \tag{D3}$$

where $\mathrm{Re}\{\boldsymbol{\mathcal{H}}\} = (\boldsymbol{\mathcal{H}} + \boldsymbol{\mathcal{H}}^*)/2$. *If $\boldsymbol{W}$ is orthogonal with $\boldsymbol{W} = (\vec{w}_1, \vec{w}_2, \dots)^\top$, then we rewrite the QFI matrix as*

$$(\boldsymbol{\mathcal{F}}_Q(\Xi))_{IJ} = \begin{cases} 4\left(\vec{w}_I^\top\boldsymbol{\mathcal{H}}\vec{w}_I\right), & I = J \\ 8\mathscr{C}_{IJ}(\vec{w}_I^\top\,\mathrm{Re}\{\boldsymbol{\mathcal{H}}\}\vec{w}_J), & I \neq J \end{cases}. \tag{D4}$$

Proof. Recall the Bures distance (B10). Introduce the invertible matrix $\boldsymbol{W}$ into Eq. (3) to determine the following relations:

$$\begin{aligned} \mathrm{Tr}\{\boldsymbol{V}\boldsymbol{\mathcal{H}}\} &= \mathrm{Tr}\big\{(\boldsymbol{W}\boldsymbol{V}\boldsymbol{W}^\top)(\boldsymbol{W}^{-\top}\boldsymbol{\mathcal{H}}\boldsymbol{W}^{-1})\big\} && \text{(D5)}\\ &= \mathrm{Tr}\big\{\boldsymbol{V}'(\boldsymbol{W}^{-\top}\boldsymbol{\mathcal{H}}\boldsymbol{W}^{-1})\big\} && \text{(D6)}\\ &= \sum_{I,J}\boldsymbol{V}'_{IJ}(\boldsymbol{W}^{-\top}\boldsymbol{\mathcal{H}}\boldsymbol{W}^{-1})_{IJ} && \text{(D7)}\\ &= \sum_{I}\xi_I^2(\boldsymbol{W}^{-\top}\boldsymbol{\mathcal{H}}\boldsymbol{W}^{-1})_{II} + \sum_{\substack{I,J\\ I\neq J}}\xi_I\xi_J\mathscr{C}_{IJ}(\boldsymbol{W}^{-\top}\boldsymbol{\mathcal{H}}\boldsymbol{W}^{-1})_{IJ}. && \text{(D8)} \end{aligned}$$

Note that $\mathscr{C}_{JI} = \mathscr{C}_{IJ}$ and $\boldsymbol{\mathcal{H}}_{JI} = \boldsymbol{\mathcal{H}}_{IJ}^*$. Substituting Eq. (D8) into the right hand side of Eq. (4) and matching like terms on both sides of the equality, we deduce that

$$(\boldsymbol{\mathcal{F}}_Q(\Xi))_{IJ} = \begin{cases} 4(\boldsymbol{W}^{-\top}\boldsymbol{\mathcal{H}}\boldsymbol{W}^{-1})_{II}, & I = J \\ 8\mathscr{C}_{IJ}(\boldsymbol{W}^{-\top}\,\mathrm{Re}\{\boldsymbol{\mathcal{H}}\}\boldsymbol{W}^{-1})_{IJ}, & I \neq J, \end{cases} \tag{D9}$$

where $\mathrm{Re}\{\boldsymbol{\mathcal{H}}\} = (\boldsymbol{\mathcal{H}} + \boldsymbol{\mathcal{H}}^*)/2$.

Furthermore, suppose that $\boldsymbol{W}$ is orthogonal such that $\boldsymbol{W}^\top = \boldsymbol{W}^{-1}$, and write $\boldsymbol{W} = (\vec{w}_1, \vec{w}_2, \dots)^\top$. Then $\boldsymbol{W}^{-\top}\boldsymbol{\mathcal{H}}\boldsymbol{W}^{-1} = \boldsymbol{W}\boldsymbol{\mathcal{H}}\boldsymbol{W}^\top$ and

$$\begin{aligned} \boldsymbol{W}\boldsymbol{\mathcal{H}}\boldsymbol{W}^\top &= \begin{pmatrix} \vec{w}_1^\top \\ \vec{w}_2^\top \\ \vdots \end{pmatrix} \boldsymbol{\mathcal{H}} \begin{pmatrix} \vec{w}_1 & \vec{w}_2 & \dots \end{pmatrix} && \text{(D10)}\\ &= \begin{pmatrix} \vec{w}_1^\top\boldsymbol{\mathcal{H}}\vec{w}_1 & \vec{w}_1^\top\boldsymbol{\mathcal{H}}\vec{w}_2 & \dots \\ \vec{w}_2^\top\boldsymbol{\mathcal{H}}\vec{w}_1 & \vec{w}_2^\top\boldsymbol{\mathcal{H}}\vec{w}_2 & \dots \\ \vdots & \vdots & \ddots \end{pmatrix}. && \text{(D11)} \end{aligned}$$

Whence, $(\boldsymbol{W}^{-\top}\boldsymbol{\mathcal{H}}\boldsymbol{W}^{-1})_{IJ} = \vec{w}_I^\top\boldsymbol{\mathcal{H}}\vec{w}_J$, which concludes the proof. □

Appendix E: Backgrounds Trigger Rayleigh's Curse

In this section, we extend our derivations to include background (e.g., thermal) fluctuations, $(\boldsymbol{\Sigma})_{ij} := \langle\Delta\lambda_i\Delta\lambda_j\rangle_{\mathrm{bkg}}$, that distinguish themselves from the desired parameters of $\boldsymbol{V}$. We assume the background fluctuations to arise from the same generators as $\boldsymbol{V}$, i.e. representing parallel decoherence [53]. Practically, such backgrounds must be characterized and subtracted off in post-processing (a common practice when measuring feeble signals, such as searches for new physics [58]). Regarding quantum limits, although backgrounds do not stymie an entanglement advantage for the correlated noise estimation problem, relatively large backgrounds do lead to the phenomenon of Rayleigh's curse [45, 86], as we demonstrate below for the multi-parameter problem.

Proposition 2. *Consider mixing background fluctuations, $\boldsymbol{\Sigma}$, into the signal, such that $\boldsymbol{V}_{ij} \to \boldsymbol{\Sigma}_{ij} + \boldsymbol{V}_{ij}$ and suppose both weak signal and weak background fluctuations. Given $\xi_I^2 := (\boldsymbol{W}\boldsymbol{V}\boldsymbol{W}^\top)_{II}$ and $\sigma_I^2 := (\boldsymbol{W}\boldsymbol{\Sigma}\boldsymbol{W}^\top)_{II}$, the QFI for the collective fluctuations $\Xi = \{\xi_I\}_{I=1}^K$ is*

$$(\boldsymbol{\mathcal{F}}_Q(\Xi;\sigma))_{II} = \left(\frac{4\xi_I^2}{\sigma_I^2 + \xi_I^2}\right)(\boldsymbol{W}\boldsymbol{\mathcal{H}}\boldsymbol{W}^\top)_{II}. \tag{E1}$$

The QFI suffers from Rayleigh's curse [45, 86]—i.e., the QFI vanishes (equivalently, the estimation error diverges) as $\xi_I \to 0$ for all probes and measurements, given $\sigma_I > 0$.

Proof sketch. Additive backgrounds, $\boldsymbol{\Sigma}$, change the noise channel to $\Phi_{\widetilde{\boldsymbol{V}}}$ with $\widetilde{\boldsymbol{V}} = \boldsymbol{\Sigma} + \boldsymbol{V}$. As before, we assume an approximate quantum channel $\Phi_{\widetilde{\boldsymbol{V}}}$, similar to Eq. (1), under the additional assumption of weak backgrounds. We then determine the QFI matrix, $\boldsymbol{\mathcal{F}}_{\mathcal{Q}}(\tilde{\Theta})$, of the new parameters $\tilde{\vartheta}_I^2 \coloneqq (\boldsymbol{W}\widetilde{\boldsymbol{V}}\boldsymbol{W}^\top)_{II} = \sigma_I^2 + \vartheta_I^2$, finding $\boldsymbol{\mathcal{F}}_{\mathcal{Q}}(\tilde{\Theta}) = 4(\boldsymbol{W}\boldsymbol{\mathcal{H}}\boldsymbol{W}^\top)_{II}$. Finally, we use $\frac{\partial\tilde{\vartheta}_I}{\partial\vartheta_J} = \delta_{IJ}(\vartheta_J/\tilde{\vartheta}_J)$ and apply the error propagation rule to reckon $\boldsymbol{\mathcal{F}}_{\mathcal{Q}}(\Theta) = \left|\frac{\partial\tilde{\vartheta}_I}{\partial\vartheta_I}\right|^2 \boldsymbol{\mathcal{F}}_{\mathcal{Q}}(\tilde{\Theta})$. □

Rayleigh's curse applies equally to the single-parameter estimation problems considered in the main text, i.e. for $\boldsymbol{V} = g^2\boldsymbol{v}$. This fact follows the same line of reasoning as Proposition 2, but we spell out the details for clarity.

Let $\widetilde{\boldsymbol{V}} = \boldsymbol{V} + \boldsymbol{\Sigma}$, where $\boldsymbol{V} = g^2\boldsymbol{v}$ and $\boldsymbol{v} = \mathrm{Tr}\{\boldsymbol{v}\}\vec{v}\vec{v}^\top$. Define the new parameter $\tilde{\vartheta} \coloneqq (\vec{v}^\top\widetilde{\boldsymbol{V}}\vec{v})^{1/2} = (g^2\,\mathrm{Tr}\{\boldsymbol{v}\} + \sigma^2)^{1/2}$, where $\sigma^2 \coloneqq \vec{v}^\top\boldsymbol{\Sigma}\vec{v}$ denotes background fluctuations projected onto the $\vec{v}$ mode. To derive the QFI for g, we first find the QFI for $\tilde{\vartheta}$, which is simply $\mathcal{F}_{\mathcal{Q}}(\tilde{\vartheta}) = 4(\vec{v}^\top\boldsymbol{\mathcal{H}}\vec{v})$. Using the error propagation rule for the Fisher information and the fact that $\partial\tilde{\vartheta}/\partial g = g\,\mathrm{Tr}\{\boldsymbol{v}\}/\tilde{\vartheta}$, it follows that

$$
\begin{aligned}
\mathcal{F}_{\mathcal{Q}}(g) &= \left|\frac{\partial\tilde{\vartheta}}{\partial g}\right|^2 \mathcal{F}_{\mathcal{Q}}(\tilde{\vartheta}) && \text{(E2)}\\
&= \left(\frac{g^2\,\mathrm{Tr}\{\boldsymbol{v}\}^2}{g^2\,\mathrm{Tr}\{\boldsymbol{v}\} + \sigma^2}\right) 4(\vec{v}^\top\boldsymbol{\mathcal{H}}\vec{v}) && \text{(E3)}\\
&= \left(\frac{g^2\,\mathrm{Tr}\{\boldsymbol{v}\}}{g^2\,\mathrm{Tr}\{\boldsymbol{v}\} + \sigma^2}\right) 4\,\mathrm{Tr}\{\boldsymbol{v}\boldsymbol{\mathcal{H}}\}. && \text{(E4)}
\end{aligned}
$$

To arrive at the final equality, we used $\mathrm{Tr}\{\boldsymbol{v}\boldsymbol{\mathcal{H}}\} = \mathrm{Tr}\{\boldsymbol{v}\}\vec{v}^\top\boldsymbol{\mathcal{H}}\vec{v}$. Hence, the emergence of Rayleigh's curse. We note that, since the QFI still scales with the global quantity $\mathrm{Tr}\{\boldsymbol{v}\boldsymbol{\mathcal{H}}\}$, we nonetheless maintain an entanglement advantage over separable strategies, which differs from unitary estimation in the presence of (parallel) background decoherence [53–55].